Journal Pre-proof

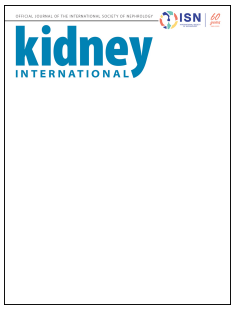

The role of desmoglein-2 in kidney disease

Tong Xu, MD, Lea Herkens, Ting Jia, MD, Barbara M. Klinkhammer, PhD, Sebastian Kant, PhD, Claudia A. Krusche, Ass. Prof., PhD, Eva M. Buhl, PhD, Sikander Hayat, PhD, Jürgen Floege, Prof., MD, Pavel Strnad, Prof., MD, Rafael Kramann, Prof. MD, PhD, Sonja Djudjaj, Ass. Prof., PhD, Peter Boor, Prof., MD, PhD

PII: S0085-2538(24)00120-0

DOI: https://doi.org/10.1016/j.kint.2024.01.037

Reference: KINT 3754

To appear in: *Kidney International*

Received Date: 8 November 2022

Revised Date: 7 December 2023

Accepted Date: 9 January 2024

Please cite this article as: Xu T, Herkens L, Jia T, Klinkhammer BM, Kant S, Krusche CA, Buhl EM, Hayat S, Floege J, Strnad P, Kramann R, Djudjaj S, Boor P, The role of desmoglein-2 in kidney disease, *Kidney International* (2024), doi: https://doi.org/10.1016/j.kint.2024.01.037.

The role of desmoglein-2 in kidney disease

kidney INTERNATIONAL
ISN INTERNATIONAL SOCIETY OF NEPHROLOGY

Hypothesis: Dsg2 might have protective effects in kidney diseases

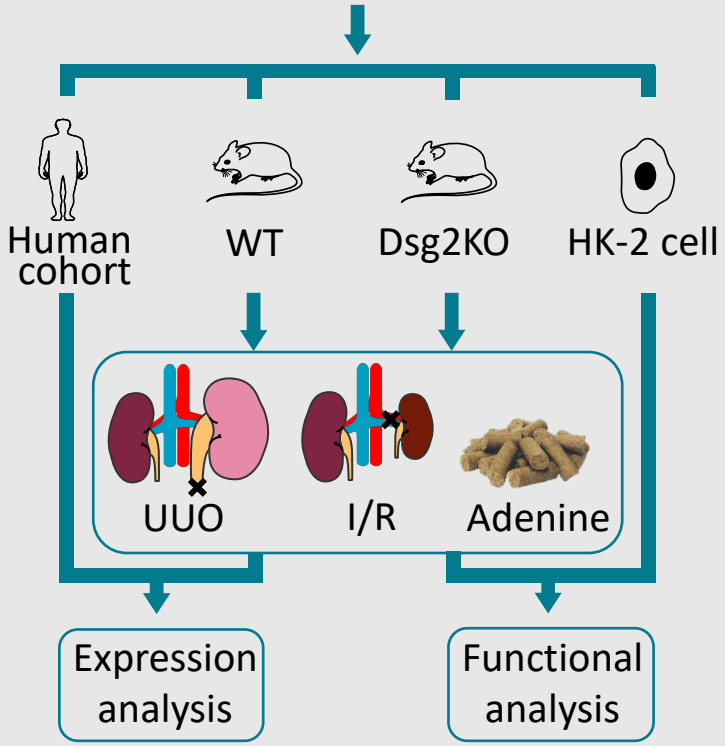

Results: Expression analysis

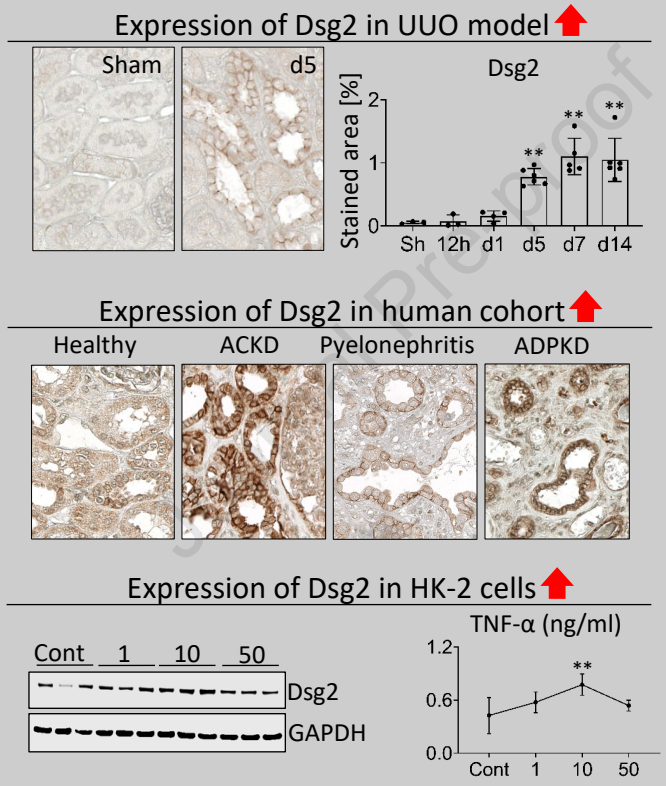

Results: Functional analysis

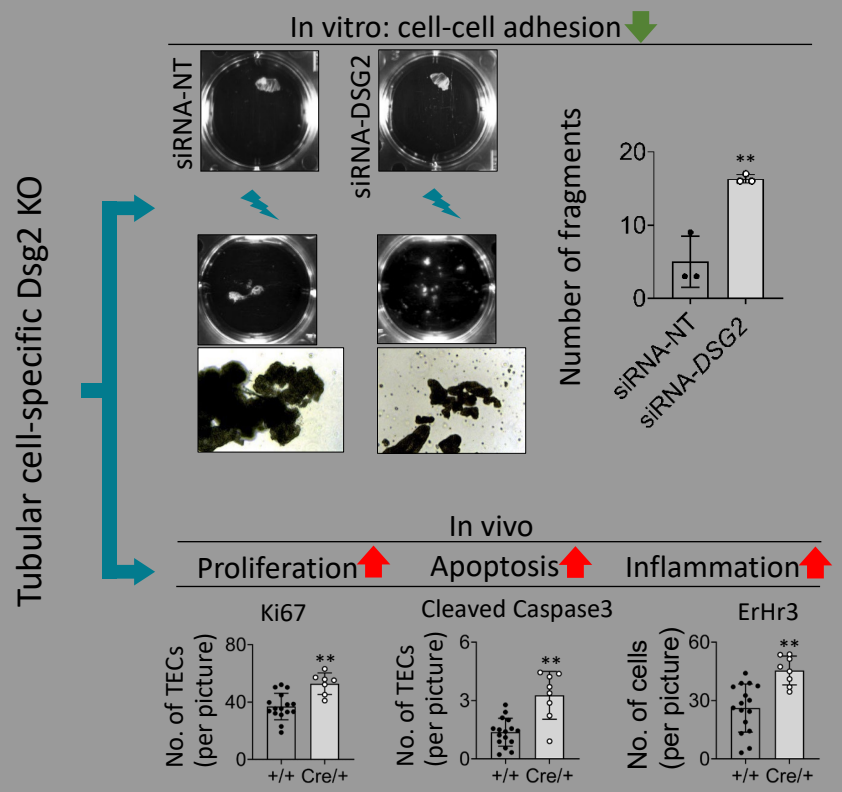

Xu and Herkens et al, 2024

Conclusion:
Desmosomal components were upregulated in tubular epithelial cells across species and diseases and protected tubular cells from injury and mechanical stress in different models of tubular damage.

[QUERY TO AUTHOR: title and abstract rewritten by Editorial Office – not subject to change]

The role of desmoglein-2 in kidney disease

Authors: Tong Xu[1,2*], Lea Herkens[1*], Ting Jia[1,6], Barbara M. Klinkhammer[1], Sebastian Kant[3], Claudia A. Krusche[3], Eva M. Buhl[7], Sikander Hayat[8], Jürgen Floege[4], Pavel Strnad[5], Rafael Kramann[4,8,9], Sonja Djudjaj[1 *], Peter Boor[1,4,7 * #]

Author affiliation:

1. Institute of Pathology, RWTH Aachen University, Aachen, Germany
2. Department of Urology, The First Affiliated Hospital of Airforce Medical University, Xi'an, China
3. Institute of Molecular and Cellular Anatomy, RWTH Aachen University, Aachen, Germany
4. Division of Nephrology and Clinical Immunology, RWTH Aachen University, Aachen, Germany
5. Department of Medicine III, Gastroenterology, Metabolic Diseases and Intensive Care, RWTH Aachen University, Aachen, Germany
6. Department of Nephrology, The Second Affiliated Hospital of Xi'an Jiaotong University, Xi'an, China.
7. Electron Microscopy Facility, RWTH Aachen University, Aachen, Germany
8. Institute of Experimental Medicine and Systems Biology, RWTH Aachen University, Aachen, Germany.
9. Department of Internal Medicine, Nephrology and Transplantation, Erasmus Medical Center, Rotterdam, Netherlands.

Academic title for authors:

Tong Xu: MD
Lea Herkens
Ting Jia: MD
Barbara Mara Klinkhammer: PhD
Sebastian Kant: PhD
Claudia Astrid Krusche: Ass. Prof.,PhD
Eva Miriam Buhl: PhD
Pavel Strnad: Prof., MD
Sikander Hayat: PhD
Jürgen Floege: Prof., MD
Rafael Kramann: Prof. MD, PhD
Sonja Djudjaj: Ass. Prof., PhD
Peter Boor: Prof., MD, PhD

*** Shared first and last authorship**

 # Address correspondence to:

Peter Boor, MD, PhD

Institute of Pathology
RWTH Aachen University Hospital
Pauwelsstrasse 30
52074 Aachen, Germany
Phone: +49 241 80 85227
Fax: +49 241 80 82446
E-mail: pboor@ukaachen.de

Funding: The study was supported by the German Research Foundation (DFG, Project IDs 322900939 & 454024652 to PB, 432698239 to PB & SD and 445703531 to PB & SD & BMK), European Research Council (ERC Consolidator Grant No 101001791 to PB), and the Federal Ministry of Education and Research (BMBF, STOP-FSGS-01GM1901A to PB and SD). PS is supported by the DFG (STR1095/6–1).

Running head: Desmoglein-2 in kidney disease

Abstract

Desmosomes are multi-protein cell-cell adhesion structures supporting cell stability and mechanical stress resilience of tissues; best described in skin and heart. The kidney is exposed to various mechanical stimuli and stress, yet little is known about kidney desmosomes. In healthy kidneys, we found desmosomal proteins located at the apical-junctional complex in tubular epithelial cells. In four different animal models and patient biopsies with various kidney diseases, desmosomal components were significantly upregulated and partly miss-localized outside of the apical-junctional complexes along the whole lateral tubular epithelial cell membrane. The most upregulated component was desmoglein-2 (Dsg2). Mice with constitutive tubular epithelial cell-specific deletion of *Dsg2* developed normally and other desmosomal components were not altered in these mice. When challenged with different types of tubular epithelial cell injury (unilateral ureteral obstruction, ischemia-reperfusion, and 2,8-dihydroxyadenine crystal nephropathy) we found increased tubular epithelial cell apoptosis, proliferation, tubular atrophy, and inflammation compared to wild type mice in all models and time points. *In vitro*, silencing *DSG2* via siRNA weakened cell-cell adhesion in HK-2 cells and increased cell death. Thus, our data show a prominent upregulation of desmosomal components in tubular cells across species and diseases and suggest a protective role of Dsg2 against various injurious stimuli.

Keywords

Desmosome, kidney tubular epithelial cells, mechanical stress, kidney injury

Translational statement

We have found a significant upregulation of desmosomal components in kidney tubular cells in various preclinical disease models and patient biopsies, the most prominent being Desmoglein-2 (Dsg2). In genetically modified animals with tubular cell-specific deletion of *Dsg2*, we found that *Dsg2* was dispensable for normal kidney development, but its deletion aggravated kidney tubular injury and inflammation in various disease models and weakened cell-cell connection. Our data support the role of mechanical stress in the pathogenesis of kidney diseases and uncover a novel molecular mechanism protecting tubular cells from injury.

Introduction

Kidney tubular epithelial cells (TEC) represent the largest cell population in the kidneys and are essential for normal kidney function. TEC are known to react sensitively to many injurious stimuli, such as hypoxia, crystals, toxins, or inflammation. Acute TEC injury is a common pathological finding in kidney biopsies and the main pathological correlate of acute kidney injury [1].

Desmosomes are cell-cell adhesion structures serve as anchors for the cytoplasmic intermediate filament cytoskeleton, providing tissues with mechanical coherence and stability [2, 3]. Desmosomes are multi-protein complexes comprising the cytoskeleton-associated protein desmoplakin (Dsp), which directly binds to the cytoplasmic intermediate filaments in the inner dense desmosomal plaque. This binding is further stabilized by the armadillo protein family which consists of plakoglobin (Pg) and plakophilin (Pkp1-4). Pg and Pkp bind to two intercellular cadherin protein families, i.e., desmoglein (Dsg1-4) and desmocollin (Dsc1-3) that bridge the extracellular space and interact with each other to mediate the connection to adjacent cells. Dsg2 and Dsc2 are the most abundant members of desmosomal cadherins in simple epithelia [4-7].

The role of desmosome is best described in the skin and the heart, i.e., organs constantly exposed to mechanical stress. Studies showed that autoantibodies against Dsg1 and Dsg3 lead to pemphigus vulgaris and pemphigus foliaceous in the skin, severe blistering diseases of the skin and the mucosa [8, 9]. Mutations in *DSG2*, *PKP2* or *DSP* result in arrhythmogenic right ventricular cardiomyopathy possibly due to impaired cell-cell adhesion. Some desmosomal components，e.g. Dsg2, were also described to be involved in regulating proliferation, apoptosis, migration, and inflammation [10-15].

Previously we have shown that keratins, the intermediate filaments of the TEC cytoskeleton which are anchored to desmosomes, were prominently upregulated in stress situations in TEC in a wide range of kidney diseases [16]. Furthermore, mislocalization of desmosomal proteins was noted in autosomal dominant polycystic kidney disease (ADPKD) [17, 18]. The desmosomal proteins Dsp, Dsg1 and Dsc2 were found to be expressed in TEC in the developing kidneys of humans and mice [19].

However, no data are available on the expression, regulation, and functional role of desmosomes and desmosomal components in other kidney diseases.

Here we comprehensively characterized the expression and regulation of different desmosomal components in healthy kidneys and different kidney diseases in preclinical models and patient biopsies and analyzed the functional consequences of tubular cell deletion of Dsg2 in transgenic mice.

Methods

Study design and ethics

Human kidney samples were collected from biopsy and resection specimens of the Institute of Pathology of the University Clinic RWTH Aachen. All samples were handled anonymously, and the study was approved by the local review board (EK244/14 and EK042/17) and in line with the Declaration of Helsinki. In total thirty-four patient kidney samples were included in the study, involving healthy human kidneys (n=5), renovascular disease (n=2), pyelonephritis (n=5), hydronephrosis/nephrolithiasis (n=5), acquired cystic kidney disease (ACKD) (n=6), autosomal dominant polycystic kidney disease (ADPKD) (n=5) and T-cells mediated rejection injury (n=5). Patient characteristics showed in Table 1 and Supplementary Figure S1.

Animal experiments: In total 33 C57Bl/6N wild type male mice, 28 *Pax8-Cre::Dsg2*$^{flox/flox}$ male mice, 23 *Pax8-Cre::Dsg2*$^{flox/flox}$ female mice, 43 wild type male littermates and 26 wild type female littermates (all animals age 10-14 weeks old, except the mice or the aging experiment) were employed and induced to the below-mentioned disease models. The animals were kept in animal facility of the University hospital RWTH Aachen with constant temperature, humidity and 12-hour light-dark cycles. Tap water and standad chow were freely accessible. Each mouse has an individual ID number and detailed records were kept of its rearing, grouping, surgical records, sampling and data analysis. Mice were randomly assigned to each group and excluded if there were any problems during surgery and no damage was visible in the PAS staining. The Sample size was determined based on the number of experimental groups and different analysis time points. Animals of the same sex, age and body weight were

divided into groups for comparison. The operation was performed by the same experienced member. In this way experimental error is reduced. Every effort was made to minimize animal suffering and all animal experiments were approved by the local government authorities (*Landesamt für Natur, Umwelt und Verbraucherschutz Nordrhein-Westfalen*).

Unilateral ureteral obstruction model (UUO)

In the UUO model, the left ureter was ligated by electro-cauterization as described previously [16]. As controls (sham, n=3), mice underwent the same surgery procedure except for the ureter ligation step. Following time points were performed in male C57Bl/6N wild type mice: UUO 12 hours (n=4), day 1 (n=4), day 5 (n=6), day 7 (n=5), day 14 (n=6) and day 21 (n=4). In a second approach, UUO day 5 and day 10 were performed in male *Pax8-Cre::Dsg2*$^{flox/flox}$ (day5: n=9; day 10: n=8) and wild type littermates (day 5: n=8, day 10: n=16).

Ischemia-reperfusion model (I/R)

We used female *Pax8-Cre::Dsg2*$^{flox/flox}$ (n=8) and wild type littermates (n=13) for this model. I/R was performed by clamping the left renal artery with a micro-serrefine clip for 35 minutes as previously described [20]. A heating blanket was used during the surgical procedure to keep a constant temperature of 37°C. Kidneys were harvested on day 21 after the surgery.

Bilateral Ischemia-reperfusion model (bil/R)

Bil/R was performed in male *Pax8-Cre::Dsg2*$^{flox/flox}$ (n=8) and wild type littermates (n=16) by clamping the left and right renal artery with a micro-serrefine clip for 25 min. During the surgical procedure a constant temperature of 37°C was kept and the mice have been sacrificed after 24h. Urine was collected before the operation and 6h before the sacrifice.

2,8-dihydroxyadenine nephropathy model (Adenine)

186 This model was performed in female *Pax8-Cre::Dsg2*$^{flox/flox}$ (n=10) and wild type
187 littermates (n=9) and induced by administration of an adenine-rich diet (supplemented
188 with 0.2% adenine). All mice had free access to adenine chow and water *ad libitum* as
189 previously described [21]. The mice were sacrificed 14 days after starting the adenine
190 diet and kidney, urine and serum were collected.
191

192 **Other methods**

193 All other methods used in this study can be found in the supplementary information,
194 i.e., *in vitro* cell culture experiments, histology, immunohistochemistry and
195 immunofluorescence, RNA extraction and analysis, Western blot analysis, public array
196 analysis, digital data analysis and single cell RNA sequencing.
197

198 **Statistical analysis**

199 The sample size of each group included at least three animals. All statistical analyses
200 were performed using GraphPad Prism 8.3.0 (LaJolla, USA). Data are presented as
201 mean ± standard deviation (SD). The two-tailed unpaired Student's t-test was applied
202 for the comparison of two groups. One-way analysis of variance (one-way ANOVA)
203 with Turkey correction was used for the comparison of multiple groups. Statistical
204 significance was defined as $p<0.05$. The adj. P-value in the publicly available datasets
205 were provided by the online datasets. The acceptable error rate is 5%.
206

207 **Results**

208 **Expression of desmosomal proteins in kidneys**

209 First, we confirmed the localization of the desmosomes in healthy murine and human
210 kidney TEC by electron microscopy, showing that the typical desmosomal structures
211 were predominantly localized at the apical-junction complexes directly beneath tight
212 and adherens junctions (Figure 1a,b). In kidney diseases, we observed an increased
213 number of desmosomes in both mice and humans (Figure 1c,d). Analysis of single-cell
214 RNA sequencing (scRNA-seq) data from human kidneys [22] confirmed the expression

215 of mRNA of desmosomal components mainly in TEC, with particularly strong
216 expression of *DSG2* (Supplementary Figure S2).
217 In healthy mice, the expression of nearly all members of desmosomal proteins was
218 confined to TEC, localized at the apical-lateral cell membrane (Figure 1e-n highlighted
219 by arrowheads). Murine hearts [23-28] (Supplementary Figure S3a-i) and skin [8, 9, 28, 29]
220 (Supplementary Figure S3a'-i') were used as positive controls to confirm the specificity
221 of the antibody staining, and non-specific IgG (Supplementary Figure S3j and j') was
222 used as a negative control.
223

224 **Regulation of Dsg2 in kidney diseases**

225 We next analyzed the regulation of the desmosomal components during disease in the
226 publicly available datasets in the Gene Expression Omnibus (GEO) database using
227 the Geo2R tool. Compared to healthy mice, an up-regulation of several desmosomal
228 genes, especially *Dsg2,* was detected in different kidney disease models
229 (Supplementary Figure S4). Then we reanalyzed our published scRNA-seq data sets
230 from human kidneys for the expression of desmosomal components in TEC [22]. We
231 observed an up-regulation of *DSG2* in injured TEC in the kidneys of patients with
232 chronic kidney disease (CKD) compared to healthy controls (Supplementary Figure
233 S5). In a time course of the murine unilateral ureteral obstruction (UUO) model [16]
234 (Supplementary Figure S6), we found a significant up-regulation of Dsg2 by
235 immunohistochemistry (Figure 2a-g), Western blot (Figure 2h-i) and RT-qPCR (Figure
236 2j). Morphologically, in disease, Dsg2 expression was localized along the entire lateral
237 membrane, suggesting aberrant localization outside of the apical-junctional complexes.
238 In addition, *in vitro* studies with the human tubular epithelial cell line HK-2 showed
239 significantly increased Dsg2 expression after challenge with TNF-α (Figure 2l-m) and
240 particularly with IFN-γ (Figure 2n-o). The expression of other desmosomal components,
241 i.e., Dsp, Dsg1 and Pg was also significantly increased after UUO (Supplementary
242 Figure S7).
243 We next analyzed three additional murine models with different types of kidney injury,
244 i.e., i) Alport mice, a transgenic model with *Col4* gene mutation leading to

245 glomerulopathy with secondary tubular injury, mimicking the human Alport syndrome,
246 ii) ischemia-reperfusion injury (I/R) as a model of acute tubular injury and iii) the 2, 8-
247 dihydroxyadenine nephropathy modeling crystal-induced TEC injury. Compared to
248 healthy kidneys, the analyzed desmosomal components, i.e., Dsc1, Dsc2, Dsc3, Dsg1,
249 Dsg2, Pkp2, Pkp3, Dsp and Pg, were all up-regulated in these models, particularly in
250 the diseased dilated tubules (Supplementary Figure S8).
251 Co-stainings with tubular segment-specific markers, such as CD13 and DBA (*Dolichos*
252 *biflorus* agglutinin), and scRNA-seq data demonstrated that Dsg2 was mainly
253 expressed by collecting ducts, distal tubules, descending thin and thick ascending limb,
254 only weakly detectable in proximal tubular cells (Figure S9), and strongly expressed in
255 injured tubules (Figure S9 c,g). We have analyzed the amount of Dsg2 using
256 immunohistochemistry in human kidney biopsies and resection specimens with various
257 kidney diseases. DSG2 was rarely detected in healthy human kidneys, while it was
258 significantly expressed during various diseases, i.e., T-cell mediated rejection,
259 pyelonephritis, autosomal dominant polycystic kidney disease (ADPKD),
260 hydronephrosis/nephrolithiasis, renovascular disease and acquired cystic kidney
261 disease (ACKD) (Figure 3a-h).
262

263 **Tubular-specific deletion of *Dsg2* did not affect the expression of other**
264 **desmosomal proteins and did not result in spontaneous tubular damage**

265 To study the functional role of Dsg2, we have established a genetic mouse model with
266 kidney TEC-specific deletion of *Dsg2* under the Pax8 promoter, the constitutive
267 $Pax8^{Cre/+}::Dsg2^{flox/flox}$ mouse (Cre/+) (Supplementary Figure S10a). The successful
268 deletion of *Dsg2* was verified by immunofluorescence staining (Supplementary Figure
269 S10b-g) and Western blot analysis (Supplementary Figure S10h). Although
270 desmosomal components were described to be expressed in embryonic kidneys [19],
271 mice with TEC-specific *Dsg2* deletion developed normally without an obvious
272 spontaneous phenotype (Supplementary Figure S10i-l). Kidney expression of other
273 desmosomal components, i.e., Dsp and Dsg1, did not change in TEC-specific *Dsg2*
274 knock-out mice (Supplementary Figure S10m-o). Kidney function was not altered and

275 also other organs, i.e., heart, intestine, liver, lung, skin, spleen or tongue showed no
276 obvious pathologic abnormalities (Supplementary Figure S11).
277 In 2,8-dihydroxyadenine nephropathy model, the kidney function showed no
278 differences after knockout *Dsg2* (Supplementary Figure S12). These data suggested
279 that Dsg2 is dispensable for normal kidney development and physiological functions.
280

281 **Tubular-specific deletion of *Dsg2* increased tubular injury and atrophy in disease**
282 **models.** The establishment of renal disease animal models is conducive to the study
283 of the relationship between the pathogenesis of renal disease, changes in tissue
284 morphology, ecological indicators and clinical manifestations. To understand the role
285 of Dsg2 in kidney disease pathophysiology, we challenged *Pax8*$^{Cre/+}$*::Dsg2*$^{flox/flox}$ mice
286 and wild type littermates with three well-established kidney injury models: UUO, I/R
287 and 2,8-dihydroxyadenine nephropathy.
288 Our data showed that after 5 days of UUO (Figure 4a), Ki67^{+} TEC significantly
289 increased up to 1.4-fold (Figure 4b-b'') and the number of cleaved caspase3^{+} TEC
290 (Figure 4c-c'') up to 1.6-fold in TEC-specific *Dsg2* knock-out mice compared to their
291 wild type littermates. The number of Er-Hr3^{+} infiltrating immune cells also significantly
292 increased in *Pax8*$^{Cre/+}$*::Dsg2*$^{flox/flox}$ mice (Figure 4d-d''). The expression of the tubular
293 injury marker Ngal did not differ between both groups (Figure 4e-e''). In a more
294 advanced disease stage after 10 days of UUO (Figure 4f), transgenic mice lacking
295 tubular *Dsg2* showed significant increase in Ki67^{+} (Figure 4g-g'') and cleaved
296 caspase3^{+} TEC (Figure 4h-h''), as well as an increase in infiltrating Er-Hr3^{+} immune
297 cells (Figure 4i-i''). Further a 2-fold increase in Ngal^{+} stained area (Figure 4j-j'') was
298 detectable. Numerically, the increase was more prominent after 10 days than after 5
299 days of UUO. The total number of tubules (Supplementary Figure 13a), the total
300 number of TECs (Supplementary Figure 13b), and their ratio (Supplementary Figure
301 13c) were similar between the groups. Normalization of the number of proliferating
302 (Supplementary Figure 13d-e) and apoptotic tubular cells (Supplementary Figure 13f-
303 g) to the total number of tubules (Supplementary Figure 13d and f) or the total number
304 of tubular epithelial cells (Supplementary Figure 13e and g) confirmed the increase

305 due to Dsg2 deficiency. Consistent with the UUO findings, in unilateral I/R injury (day
306 21) and 2,8-dihydroxyadenine nephropathy (day 14) the transgenic mice showed
307 increased TEC proliferation, apoptosis and injury, as well as more inflammatory
308 infiltrates (Figure 5). In the 2,8-dihydroxyadenine nephropathy model, but not in the
309 unilateral I/R model, Er-Hr3^{+} cells and Ngal^{+} stained area were significantly increased
310 (Figure 5).

311 We investigated the effects of *Dsg2* tubular deficiency in acute kidney injury in the
312 bilateral I/R model after 24h, allowing also the analysis of kidney function. At this early
313 stage, tubular cell injury and cell death were already significantly increased in
314 *Pax8*$^{Cre/+}$*::Dsg2*$^{flox/flox}$ mice, but in contrast to later stages, TEC proliferation was
315 significantly decreased (Figure 6). To further explore the effects of a Dsg2 deletion in
316 TEC, we measured the area of tubules in the cortical region with a deep learning-based
317 histopathologic assessment. Our data showed that in the UUO model, compared to
318 the control group, more tubules in the transgenic mice were atrophic. This was more
319 prominent at the later stage of the model at day d10 (Figure 7). The tubular-specific
320 deletion of *Dsg2* increased tubular cell loss in UUOd10 analyzed by counting the
321 tubules containing cell debris in the tubular lumen (Figure 7d-d'') and the adenine
322 model by analyzing the urine for Keratin 18 and its caspase-cleaved fragment (Figure
323 7 e-g).

324 Immunofluorescence staining of tubular segments with specific markers, i.e. CD13 for
325 proximal tubules and THP for distal tubules revealed that the cell debris in the tubular
326 lumen of the Dsg2 deficient mice were THP+ (Supplementary Figure 14 a-a''). Re-
327 analysis of TEC proliferation in these two different tubular segments showed that the
328 increase in TEC proliferation is also mainly in THP+ (Supplementary Figure 14 b-e)
329 and not in CD13+ TECs (Supplementary Figure 14f-i).

330 Next, we investigated the expression of 118 different cytokines in kidneys of
331 *Pax8Cre::Dsg2*$^{flox/flox}$ mice compared to wild type littermates after 14 days of adenine
332 enriched diet. Twentyone proteins were differentially regulated in the Dsg2 deficient
333 mice, 19 up- and 2 downregulated. These included tubular injury markers Kim-1 and
334 Ngal or proinflammatory cytokines TNFα and IFNγ (Figure 7h).

335

336 **Lack of *DSG2* weakened cell connections in HK-2 cells *in vitro***

337 Using the human tubular epithelial cell line HK-2, we suppressed *DSG2* gene
338 expression *via* siRNA and confirmed the successful downregulation by Western blot
339 analysis and immunofluorescence staining (Supplementary Figure S15a-d).

340 To study the role of Dsg2 in cell adhesion, we treated the confluent cell monolayer with
341 dispase to release it from the bottom of cell culture flasks. This monolayer was then
342 subjected to shear stress by pipetting. Shear stress resulted in increased number of
343 small fragments of the original monolayer. This fragmentation was more pronounced
344 in siRNA-*DSG2* treated cells compared to the controls (Figure 8a-g), suggesting a
345 weakening of cell-cell adhesion following reduced Dsg2 expression. To analyze the
346 effect of *DSG2* deficiency on cell proliferation and cell death, HK-2 cells were
347 transfected with siRNA-*DSG2* or the control siRNA-NT and challenged with 15% FCS
348 to induce proliferation or with IFNγ or TNFα to induce cell stress/death. *DSG2*
349 deficiency led to a transient reduction of cell proliferation in a mitogenic setting (FCS
350 stimulation, Figure 8h), but to an increased proliferation under stress (induced by IFNγ
351 (8i) or TNFα (8j)). In parallel cell death was significantly higher in tubular cells lacking
352 *DSG2* (Figure 8h'-j').

353

354 **Discussion**

355 Our study is the first to comprehensively analyze the expression and regulation of
356 desmosomal components and the functional role of Dsg-2 in kidney tubular epithelial
357 cells *in vivo*. Our data is in line with the previous three reports describing the expression
358 of Dsg1 [18, 19], Dsg2 [17], Dsc2/3 [18, 19], Dsp [17-19] and Pg [17] in TEC.

359

360 The kidney tubular cell-specific *Dsg2* knockout in mice showed no obvious
361 spontaneous pathologic phenotype and no changes in kidney function. This is in line
362 with our previous study, showing that Dsg2 was not required for desmosomal assembly
363 and embryonic development in the intestine [30]. Conversely, *Dsg2* knockout in the
364 intestine enhanced intestinal epithelial barrier disruption after challenging the mice with

365 dextran sodium sulfate [30] and *Dsg2* knockout in cardiomyocytes led to the development
366 of arrhythmogenic cardiomyopathy [23-28]. This suggests that Dsg2 is essential for the
367 desmosomal function of tissues subjected to intense mechanical stress under
368 physiological conditions like the heart but is dispensable in the kidneys. In healthy
369 kidney TEC, we found a low basal expression of desmosomal proteins. This is in line
370 with studies showing low amounts of Dsg2 and Dsc2 expression in healthy mouse
371 kidneys [30] and weak Dsg1/2 in healthy human kidneys [18]. We observed increased
372 expression of the majority of desmosomal proteins during kidney disease *in vivo* in
373 both mice and patients, including Dsg2. This increase was particularly localized to
374 dilated tubules. A previous study showed that the mechanical tension on TEC was
375 increased during UUO [31, 32]. Our data suggest that the increased expression of
376 desmosomal proteins might be the response to mechanical stress. Our data showed
377 Dsg2 being mostly expressed outside the proximal tubular compartment, particularly
378 in the distal tubules and collecting ducts. Proximal tubular cells are usually considered
379 the important cells driving kidney disease inflammation and progression in the models
380 analyzed. Therefore, our data suggest that the distal tubular compartment might also
381 be important in driving the progression of the reported models, in line with some
382 previous reports [33-38]. Our data indicate that due to Dsg2 deficiency is an increased cell
383 loss and thus more regeneration/proliferation, especially in the tubular segment where
384 Dsg2 is mainly expressed, namely the distal THP+ tubules.
385 In the various diseases, we observed the expression of Dsg2 and other desmosomal
386 proteins along the whole lateral membrane of TEC. Desmosomes are normally located
387 at the apical junctional complex in TEC [4], and we also haven't observed desmosomal
388 structures in electron microscopy outside of apical-junctional complexes neither in
389 healthy nor diseased TEC. This might suggest an extra-desmosomal location of Dsg2.
390 Similar findings were described in other desmosome-rich tissues, i.e., cell membranes
391 of epithelia were strongly Dsg2-positive in the healthy intestine [30], endometrium [39] and
392 skin [40]. One study suggested that an extra-desmosomal Dsg2 on the surface of
393 polarized enterocytes regulated intestinal barrier function *via* mitogen-activated protein
394 kinase (p38MAPK) signaling *in vitro* [41]. The extra-desmosomal Dsg3 was detected in

395 keratinocytes *in vitro* and this extra-desmosomal Dsg3 could form a signaling complex
396 together with E-cadherin, β-catenin and Rous sarcoma (Src) kinase to strengthen
397 keratinocytes cohesion also *via* p38MAPK signaling [29, 42]. The exact role of extra-
398 desmosomal Dsg2 in the kidney remains unclear and will require future studies.
399
400 In our transgenic mice, we did not observe any changes in other members of the
401 desmosome such as Dsg1 or Dsp, which could potentially compensate for the lack of
402 Dsg2. Together with our findings of functional consequences of Dsg-2 deletion in TEC
403 supports the hypothesis, that other desmosomal components are not able to
404 compensate for the loss of one specific desmosomal protein [28].
405
406 In the examined disease models, *Dsg2* deletion led to several changes in TEC. The
407 observed increased TEC apoptosis *in vivo and in vitro* was similar to previous studies
408 showing cardiomyocyte apoptosis as an early finding in Dsg2-related heart disease [10].
409 Also, we previously found a higher level of cleaved caspase-1 in the intestine in mice
410 lacking *Dsg2* [30] and the absence of other components of desmosomes in the skin, i.e.,
411 Dsg1 and Dsg3, caused increased apoptosis *in vivo* [11]. Previous studies showed that
412 abnormal connections between neighboring epithelial cells or between cells and matrix
413 might lead to an increase in cell death [43] and the integrity of desmosomes is essential
414 for extruding apoptotic cells and maintaining tissue stability *in vitro* [44]. For intestinal
415 epithelial cells it was shown that for cell survival cell-cell or cell-matrix adhesion is
416 required and that loss of such cell adhesion induced epithelial cell death in part by
417 apoptosis [45]. This is supported by upregulation of chemokines, CCL28, C5a, CXCL16
418 and KC (CXCL1), that induce apoptosis. Our *in vivo* and *in vitro* data suggest a similar
419 mechanism for renal tubular epithelial cells. While our *in vitro* data were in line with the
420 *in vivo* findings, a limitation of our study is that we only used the HK-2 cell line and not
421 primary tubular cells. Increased regeneration/proliferation of TEC was another
422 alteration we observed in TEC lacking *Dsg2* during disease *in vivo*. Similar changes
423 were seen in intestinal epithelial cell-specific Dsg2 knockout mice [30]. Currently, the
424 different effects of *Dsg2* deficiency on tubular cell proliferation in early *vs.* late disease

stages *in vivo* and proliferative *vs.* stress stimulation *in vitro*, and the interplay with apoptosis, remain unclear. Possibly, the different extent and importance of cell death *vs* regeneration during the disease stages might play a role. Lastly, we observed an increased inflammatory cell infiltration in *Pax8*$^{Cre/+}$*::Dsg2*$^{flox/flox}$ mice during kidney disease. This is in line with a previous study in the intestine showing that lack of *Dsg2* caused a strong inflammatory response due to activation of pro-inflammatory cytokines IL-1β/TNF-α and IL-22- phosphorylated signal transducer [41] and activator of transcription 3 (pSTAT3) signaling [30].

We were not able to pinpoint the connection between the different effects of Dsg2 deficiency on tubular cell proliferation in early vs. late disease stages in vivo and proliferative vs. stress stimulation in vitro, and the interplay with apoptosis. We have analyzed the previously proposed signaling pathways, particularly the MAPK (analyzing p38 and ERK phosphorylation), EGFR, and STAT-3 pathways. However, none of these pathways was significantly affected in the kidney tissues, suggesting they might not be involved (data not shown). A limitation of these analyses might be that they were performed in full kidney samples so that changes in the (distal) tubular compartment could have been masked. In summary, our findings suggest that desmosomes, and particularly desmoglein-2 are dispensable for embryonic development and physiological kidney function but are upregulated in various diseases in mice and patients and protect tubular cells from injury in different models of kidney diseases.

Disclosure

The authors declare that there is nothing to disclose.

Supplementary Material

Supplementary methods

- *In vitro* cell culture and siRNA transfection
- Histology, immunohistochemistry and immunofluorescence
- RNA extraction and analysis
- Western blot analysis
- Dispase-based dissociation array

- Proliferation & cell death analysis
- Reanalysis of public arrays
- Digital data analysis
- Single cell RNA sequencing

Supplementary figures

- Supplementary Figure S1: Patient characteristics.
- Supplementary Figure S2: The expression of mRNA of desmosomal components in human kidneys analyzed using scRNA-sequencing.
- Supplementary Figure S3: The expression of desmosomal proteins in heart and skin used as positive controls for the immunohistochemistry studies.
- Supplementary Figure S4: The expression of desmosomal mRNA in animal models by reanalysis of publicly available datasets.
- Supplementary Figure S5: The expression of desmosomal mRNA in human injured kidney tubules analyzed using scRNA-sequencing.
- Supplementary Figure S6: Histological assessment of UUO confirmed expected tubular injury pattern.
- Supplementary Figure S7: Regulation of desmosomal components in the UUO model.
- Supplementary Figure S8: The expression of desmosomal proteins in I/R, Alport and Adenine murine models.
- Supplementary Figure S9: Dsg2 is predominately expressed in distal tubules and collecting ducts.
- Supplementary Figure S10 Confirmation of *Dsg2* knock out and retained composition of desmosomal components in the transgenic mice *in vivo*.
- Supplementary Figure S11: Tubular-specific knockout of Dsg2 has no influence on kidney function or other organ development.
- Supplementary Figure S12: Dsg2 deletion did not affect kidney function in adenine model.
- Supplementary Figure 13: Normalization of proliferation and apoptosis to total number of tubules and tubular epithelial cells confirmed increase due to tubular-specific Dsg2 deficiency in the UUO model.
- Supplementary Figure 14: Tubular cell-specific Dsg2 deficiency-induced cell loss and proliferation in distal tubules.
- Supplementary Figure S15: Confirmation of *Dsg2* knock out in HK-2 cells *in vitro*.

Supplementary tables

- Table S1 Incubation times and cytokine concentrations
- Table S2: Primary antibodies list
- Table S3: Secondary antibodies used for immunohistochemistry
- Table S4: Bokemeyer buffer
- Table S5: secondary antibodies used for Western blot
- Table S6: List of analyzed publicly available data sets

502 Supplementary references
503
504 Supplementary information is available on Kidney International's website
505

506 **References**

507 1. Grgic I, Campanholle G, Bijol V*, et al.* Targeted proximal tubule injury triggers interstitial
508 fibrosis and glomerulosclerosis. *Kidney Int* 2012; **82:** 172-183.
509 2. Saito M, Tucker DK, Kohlhorst D*, et al.* Classical and desmosomal cadherins at a
510 glance. *Journal of cell science* 2012; **125:** 2547-2552.
511 3. Windoffer R, Borchert-Stuhlträger M, Leube RE. Desmosomes: interconnected
512 calcium-dependent structures of remarkable stability with significant integral
513 membrane protein turnover. *Journal of cell science* 2002; **115:** 1717-1732.
514 4. Delva E, Tucker DK, Kowalczyk AP. The desmosome. *Cold Spring Harbor perspectives*
515 *in biology* 2009; **1:** a002543.
516 5. Nie Z, Merritt A, Rouhi-Parkouhi M*, et al.* Membrane-impermeable cross-linking
517 provides evidence for homophilic, isoform-specific binding of desmosomal cadherins in
518 epithelial cells. *Journal of biological chemistry* 2011; **286:** 2143-2154.
519 6. Hatzfeld M. Plakophilins: Multifunctional proteins or just regulators of desmosomal
520 adhesion? *Biochimica Et Biophysica Acta-Molecular Cell Research* 2007; **1773:** 69-77.
521 7. Bass-Zubek AE, Godsel LM, Delmar M*, et al.* Plakophilins: multifunctional scaffolds for
522 adhesion and signaling. *Curr Opin Cell Biol* 2009; **21:** 708-716.
523 8. Spindler V, Waschke J. Pemphigus—a disease of desmosome dysfunction caused by
524 multiple mechanisms. *Frontiers in immunology* 2018; **9:** 136.
525 9. Vielmuth F, Walter E, Fuchs M*, et al.* Keratins regulate p38MAPK-dependent
526 desmoglein binding properties in pemphigus. *Frontiers in immunology* 2018; **9:** 528.
527 10. Ng K-E, Delaney PJ, Thenet D*, et al.* Early cardiac inflammation as a driver of murine
528 model of Arrhythmogenic Cardiomyopathy. *bioRxiv* 2020.
529 11. Schmidt E, Waschke J. Apoptosis in pemphigus. *Autoimmunity Reviews* 2009; **8:** 533-
530 537.
531 12. Kamekura R, Kolegraff K, Nava P*, et al.* Loss of the desmosomal cadherin desmoglein-
532 2 suppresses colon cancer cell proliferation through EGFR signaling. *Oncogene* 2014;
533 **33:** 4531-4536.
534 13. Overmiller AM, McGuinn KP, Roberts BJ*, et al.* c-Src/Cav1-dependent activation of the
535 EGFR by Dsg2. *Oncotarget* 2016; **7:** 37536.
536 14. Pilichou K, Thiene G, Bauce B*, et al.* Arrhythmogenic cardiomyopathy. *Orphanet*
537 *Journal of Rare Diseases* 2016; **11**.
538 15. Lubos N, van der Gaag S, Gercek M*, et al.* Inflammation shapes pathogenesis of
539 murine arrhythmogenic cardiomyopathy. *Basic Res Cardiol* 2020; **115:** 42.
540 16. Djudjaj S, Papasotiriou M, Bülow RD*, et al.* Keratins are novel markers of renal
541 epithelial cell injury. *Kidney Int* 2016; **89:** 792-808.
542 17. Silberberg M, Charron AJ, Bacallao R*, et al.* Mispolarization of desmosomal proteins
543 and altered intercellular adhesion in autosomal dominant polycystic kidney disease.
544 *American Journal of Physiology-Renal Physiology* 2005; **288:** F1153-F1163.
545 18. Russo RJ, Husson H, Joly D*, et al.* Impaired formation of desmosomal junctions in

546 ADPKD epithelia. *Histochem Cell Biol* 2005; **124:** 487-497.
547 19. Garrod D, Fleming S. Early expression of desmosomal components during kidney
548 tubule morphogenesis in human and murine embryos. *Development* 1990; **108:** 313-
549 321.
550 20. Buhl EM, Djudjaj S, Babickova J*, et al.* The role of PDGF-D in healthy and fibrotic
551 kidneys. *Kidney Int* 2016; **89:** 848-861.
552 21. Klinkhammer BM, Djudjaj S, Kunter U*, et al.* Cellular and molecular mechanisms of
553 kidney injury in 2, 8-dihydroxyadenine nephropathy. *Journal of the American Society of*
554 *Nephrology* 2020; **31:** 799-816.
555 22. Kuppe C, Ibrahim MM, Kranz J*, et al.* Decoding myofibroblast origins in human kidney
556 fibrosis. *Nature* 2021; **589:** 281-286.
557 23. Lahtinen AM, Lehtonen E, Marjamaa A*, et al.* Population-prevalent desmosomal
558 mutations predisposing to arrhythmogenic right ventricular cardiomyopathy. *Heart*
559 *rhythm* 2011; **8:** 1214-1221.
560 24. Asimaki A, Syrris P, Wichter T*, et al.* A novel dominant mutation in plakoglobin causes
561 arrhythmogenic right ventricular cardiomyopathy. *The American Journal of Human*
562 *Genetics* 2007; **81:** 964-973.
563 25. Fernandes MP, Azevedo O, Pereira V*, et al.* Arrhythmogenic right ventricular
564 cardiomyopathy with left ventricular involvement: a novel splice site mutation in the
565 DSG2 gene. *Cardiology* 2015; **130:** 159-161.
566 26. Wang L, Liu S, Zhang H*, et al.* Arrhythmogenic cardiomyopathy: Identification of
567 desmosomal gene variations and desmosomal protein expression in variation carriers.
568 *Experimental and therapeutic medicine* 2018; **15:** 2255-2262.
569 27. Kant S, Holthöfer B, Magin TM*, et al.* Desmoglein 2–dependent arrhythmogenic
570 cardiomyopathy is caused by a loss of adhesive function. *Circulation: Cardiovascular*
571 *Genetics* 2015; **8:** 553-563.
572 28. Najor NA. Desmosomes in human disease. *Annual Review of Pathology: Mechanisms*
573 *of Disease* 2018; **13:** 51-70.
574 29. Waschke J, Spindler V. Desmosomes and extradesmosomal adhesive signaling
575 contacts in pemphigus. *Medicinal research reviews* 2014; **34:** 1127-1145.
576 30. Gross A, Pack LA, Schacht GM*, et al.* Desmoglein 2, but not desmocollin 2, protects
577 intestinal epithelia from injury. *Mucosal immunology* 2018; **11:** 1630-1639.
578 31. Rohatgi R, Flores D. Intra-tubular hydrodynamic forces influence tubulo-interstitial
579 fibrosis in the kidney. *Current opinion in nephrology and hypertension* 2010; **19:** 65.
580 32. Quinlan MR, Docherty NG, Watson RWG*, et al.* Exploring mechanisms involved in renal
581 tubular sensing of mechanical stretch following ureteric obstruction. *American Journal*
582 *of Physiology-Renal Physiology* 2008; **295:** F1-F11.
583 33. Nam SA, Kim WY, Kim JW*, et al.* Autophagy attenuates tubulointerstital fibrosis through
584 regulating transforming growth factor-β and NLRP3 inflammasome signaling pathway.
585 *Cell Death Dis* 2019; **10**.
586 34. Cachat F, Lange-Sperandio B, Chang AY*, et al.* Ureteral obstruction in neonatal mice
587 elicits segment-specific tubular cell responses leading to nephron loss. *Kidney Int* 2003;
588 **63:** 564-575.
589 35. Gao C, Zhang L, Chen EN*, et al.* Aqp2 Progenitor Cells Maintain and Repair Distal

590 Renal Segments. *Journal of the American Society of Nephrology* 2022; **33:** 1357-1376.
591 36. Lee SY, Shin JA, Kwon HM*, et al.* Renal ischemia-reperfusion injury causes intercalated
592 cell-specific disruption of occludin in the collecting duct. *Histochem Cell Biol* 2011; **136:**
593 637-647.
594 37. Denic A, Gaddam M, Moustafa A*, et al.* Tubular and Glomerular Size by Cortex Depth
595 as Predictor of Progressive CKD after Radical Nephrectomy for Tumor. *J Am Soc*
596 *Nephrol* 2023; **34:** 1535-1545.
597 38. Ren J, Rudemiller NP, Wen Y*, et al.* The transcription factor Twist1 in the distal nephron
598 but not in macrophages propagates aristolochic acid nephropathy. *Kidney Int* 2020; **97:**
599 119-129.
600 39. Buck VU, Hodecker M, Eisner S*, et al.* Ultrastructural changes in endometrial
601 desmosomes of desmoglein 2 mutant mice. *Cell and tissue research* 2018; **374:** 317-
602 327.
603 40. Gupta A, Nitoiu D, Brennan-Crispi D*, et al.* Cell cycle-and cancer-associated gene
604 networks activated by Dsg2: evidence of cystatin A deregulation and a potential role in
605 cell-cell adhesion. *PLoS One* 2015; **10:** e0120091.
606 41. Ungewiß H, Vielmuth F, Suzuki ST*, et al.* Desmoglein 2 regulates the intestinal
607 epithelial barrier via p38 mitogen-activated protein kinase. *Scientific reports* 2017; **7:** 1-
608 10.
609 42. Rötzer V, Hartlieb E, Vielmuth F*, et al.* E-cadherin and Src associate with
610 extradesmosomal Dsg3 and modulate desmosome assembly and adhesion. *Cellular*
611 *and molecular life sciences* 2015; **72:** 4885-4897.
612 43. Valentijn A, Zouq N, Gilmore A. Anoikis. *Biochemical Society Transactions* 2004; **32:**
613 421-425.
614 44. Thomas M, Ladoux B, Toyama Y. Desmosomal junctions govern tissue integrity and
615 actomyosin contractility in apoptotic cell extrusion. *Current Biology* 2020; **30:** 682-690.
616 e685.
617 45. Nava P, Laukoetter MG, Hopkins AM*, et al.* Desmoglein-2: a novel regulator of
618 apoptosis in the intestinal epithelium. *Mol Biol Cell* 2007; **18:** 4565-4578.
619
620

621 **Acknowledgments**

622 Thanks for technical support from Simon Otten, Christina Gianussis, Louisa Böttcher,
623 Jana Baues, Marie Cherelle Timm.

624

625 **Data sharing statement:**

626 All animal studies were performed and the data generated at the University Hospital Aachen.
627 All data are available in the main text or the Supplementary Material. This article does not
628 report original code. Any additional information required to reanalyze the data reported in
629 this paper is available from the lead contact upon request. The data sets analyzed in this
630 study are available from the Gene Expression Omnibus repository under the following
631 accession numbers: GSE96101, GSE85409, GSE32583, GSE52004, GSE87023, GSE7869,
632 GSE66494, GSE30718, GSE32591. The human data were approved by the local review board

633 of the University hospital RWTH Aachen (EK244/14, EK042/17 and EK016/17), and are
634 available under restricted access for legal and privacy protection reasons, access can be
635 obtained by contacting Peter Boor, Institute of Pathology, RWTH Aachen University Clinic,
636 Aachen, Germany, (pboor@ukaachen.de). In general, the requests will be processed based
637 on institutional and national policies. Data can only be shared for non-commercial research
638 purposes and requires a data transfer agreement that is provided by the legal department of
639 the University hospital RWTH Aachen. The detailed protocol of scRNA-seq was described in a
640 previous publication (doi: 10.1038/s41586-020-2941-1).

641

642 **Figure 1: Desmosomal proteins were detected in healthy kidneys at the apico-**
643 **junctional complex (AJC).**
644 Visualization of cell-cell junctions (a-d) by electron microscopy, i.e., tight junction (TJ),
645 adherens junction (AJ) and desmosome (D) in murine and human kidney tubular
646 epithelial cells in healthy and diseased subjects. Scale bars = 500nm. Schematic
647 diagram of desmosome structure in tubular epithelial cells (e). Desmocollin (Dsc),
648 desmoglein (Dsg), plakoglobin (Pg), plakophilin (Pkp) and desmoplakin (Dsp) were
649 visualized by immunohistochemistry in healthy murine tubular epithelial cells (f-n).
650 Arrows indicate the location of the respective desmosomal component. Scale bars =
651 50µm.

652

653 **Figure 2: Expression of Dsg2 was up-regulated during stress *in vivo* and *in vitro.***
654 Dsg2 in the murine unilateral ureteral obstruction (UUO) model was significantly
655 increased at protein level analyzed by immunohistochemistry staining (a-g) and
656 immunoblotting (h, i) and at RNA level as shown by RT-qPCR (j). Scale bars = 50µm.
657 HK-2 cells were treated for 48h with different concentration of TNF-α and IFN-γ (k),
658 immunoblotting with morphometric quantification revealed a significant increase in
659 Dsg2 expression (l-o). ***: P*<0.01

660

661 **Figure 3: Expression of DSG2 was up-regulated in different human kidney**
662 **diseases.**
663 A significant increase in different human renal diseases compared to healthy controls
664 (a), i.e. arrows indicate the location of DSG2 in T-cell mediated rejection (b),
665 pyelonephritis (c), autosomal dominant polycystic kidney disease (ADPKD; d),
666 hydronephrosis due to nephrolithiasis (e), renovascular disease (f) and acquired cystic
667 kidney disease (ACKD;g) was shown by quantification of DSG2 positive stained area
668 in human kidney cortex (h). Scale bars = 50µm. ***: P*<0.01

669

670 **Figure 4: Tubular cell-specific *Dsg2* deficiency induced tubular injury and**
671 **inflammation in UUO model in mice.**
672 After 5 days of unilateral ureteral obstruction (UUO) (a), mice lacking *Dsg2* (Cre/+) in
673 tubular cells showed significant increase in Ki67$^+$ (b-b'') and cleaved caspase3$^+$ (c-c'')
674 tubular epithelial cells (TEC) and the amount of ErHr3$^+$ immune cells (d-d'') compared
675 to wild type littermates (+/+) (shown with arrowheads), while the percentage of Ngal$^+$-
676 stained area (e-e'') has not changed. At day 10 after UUO (f), Cre/+ mice showed a

significant increase in Ki67$^+$ (g-g'') and cleaved caspase3$^+$ (h-h'') TECs. In addition, more ErHr3$^+$ immune cells were seen (i-I'') (as shown by arrowheads), and a stronger tubular injury, analyzed by Ngal$^+$-stained area was detectable (j-j''). n = number. Scale bars = 50µm. ***: P* < 0.01, ns=not significant.

Figure 5: Tubular cell-specific *Dsg2* deficiency intensified tubular injury and inflammation in I/R and 2, 8-dihydroxyadenine nephropathy model in mice.
In the model of unilateral ischemia reperfusion at day 21 (I/R) (a), the TEC-specific *Dsg2* knock-out mice (Cre/+) showed a significant increase in cleaved caspase3$^+$ expression (c) in tubular epithelial cells (TECs) (arrowheads), while no difference was detectable in the amount of Ki67 positive TECs (b), Er-Hr3$^+$ immune cells (d) (as shown by arrowheads) or the Ngal positive area (e) in comparison to wild type littermates (+/+). 14 days after 2, 8-dihydroxyadenine nephropathy (Adenine) (f), the Cre/+ mice showed a significant increase in Ki67$^+$ (g) and cleaved caspase3$^+$ (h) TECs (arrowheads). In addition, the tubular-specific deletion led to an increase in the Er-Hr3$^+$ immune cell infiltration (i) (shown by arrowheads) and in tubular injury, visualized by Ngal staining (j). n = number. Scale bars = 50µm. **: P* < 0.05. ***: P* < 0.01, ns = not significant.

Figure 6: Tubular cell-specific *Dsg2* deficiency in early acute kidney injury increased tubular cell injury and tubular cell death.
Acute kidney injury (AKI) was induced by bilateral ischemia-reperfusion (biIR) for 24h (a). Mice lacking *Dsg2* (Cre/+) in tubular cells showed a significant decrease in Ki67$^+$ (b-b'') and an increase in cleaved caspase3$^+$ (c-c'') tubular epithelial cells (TEC). The amount of ErHr3+ immune cells (d-d'') compared to wild-type littermates (+/+) (shown with arrowheads) has not changed while the percentage of Ngal$^+$ area increased (e-e''). Creatinine clearance was significantly reduced in *Dsg2* deficient mice (f). *: P<0.05

Figure 7: Tubular cell-specific *Dsg2* deficiency induced tubular atrophy and tubular cell loss.
Periodic acid Schiff (PAS) staining of kidneys from wild type littermates (+/+) (a) and mice with tubular cell-specific deletion of *Dsg2* (cre/+) (b) 10 days after unilateral ureteral obstruction (UUO). Compared to wild type littermates, the size of tubules in *Dsg2* deficient mice showed no major difference between the contralateral control and the UUO-subjected kidney at day 5 group, whereas a stronger decrease in the tubular size was observed in the *Dsg2* deficient mice at UUO day 10, hinting to more tubular atrophy (c). In UUO d10 the number of tubules containing cell debris per visual field was counted (d) in wild-type littermates (d') and mice with tubular cell-specific deletion of *Dsg2* (d''). Urine analysis of full-length Keratin 18 (e) or caspase-cleaved Keratin 18 (K18) fragment (f) by Western blot (g) revealed an increase in tubular cell loss in *Dsg2* deficient mice fed for 14 days an adenine-enriched diet. Cytokine and chemokine array analysis of tissue lysats from *Dsg2* deficient mice compared to wild type littermates showed 21 differentially expressed proteins (h). Scale bars = 50µm; *: P > 0.05

Figure 8: *DSG2* knock-out promoted proliferation and reduced cell-cell-adhesion

721 **in HK-2 cells *in vitro*.**The dispase-based dissociation assay was used to evaluate the
722 strength of cell-cell adhesion. HK-2 cell sheets with (a) or without (d) DSG2 were
723 released from the cell culture dish and subjected to mechanical force as described in
724 Methods. Representative images of fragmentation induced by mechanical force (b-f).
725 The resulting fragments were counted (g). HK-2 cells with and without *DSG2* were
726 stimulated with 15% FCS (h-h'), IFNγ (i-i') or TNFα (j-j') and the number of living (h-j)
727 and dead (h'-j') cells was counted. Under proinflammatory conditions, the effect of
728 *DSG2* deficiency on cell-cell adhesion was analyzed with the dispase-based
729 dissociation assay (k). Scale bars = 100μm. *: P < 0.05. **: P < 0.01.
730
731
732 Table1: Patient characteristics

Patients' profile	Healthy group n=5	Disease group n=28	*P*
Age, mean ± SD	47.4 ± 27.2	52.5 ± 14.8	ns
Gender (%, male)	100	68	ns
Urea (mg/dl), mean ± SD	30.4 ± 9.5	81.4 ± 46.9	*P* < 0.05
Serum creatinine (mg/dl), mean ± SD	0.8 ± 0.4	5.5 ± 4.8	*P* < 0.05
eGFR, mean ± SD	67.9 ± 15.3	33.8 ± 33.6	ns
BMI, mean ± SD	21.8 ± 4.4	29.6 ± 11.9	ns

733

Table1: Patient info

Patients' profile	Healthy group n = 5	Disease group n = 28	*P*
Age, mean ± SD	47.4 ± 27.2	52.5 ± 14.8	ns
Gender (%, male)	100	68	ns
Urea (mg/dl), mean ± SD	30.4 ± 9.5	81.4 ± 46.9	$P < 0.05$
Serum creatinine (mg/dl), mean ± SD	0.8 ± 0.4	5.5 ± 4.8	$P < 0.05$
GFR, mean ± SD	67.9 ± 15.3	33.8 ± 33.6	ns
BMI, mean ± SD	21.8 ± 4.4	29.6 ± 11.9	ns

Figure 1

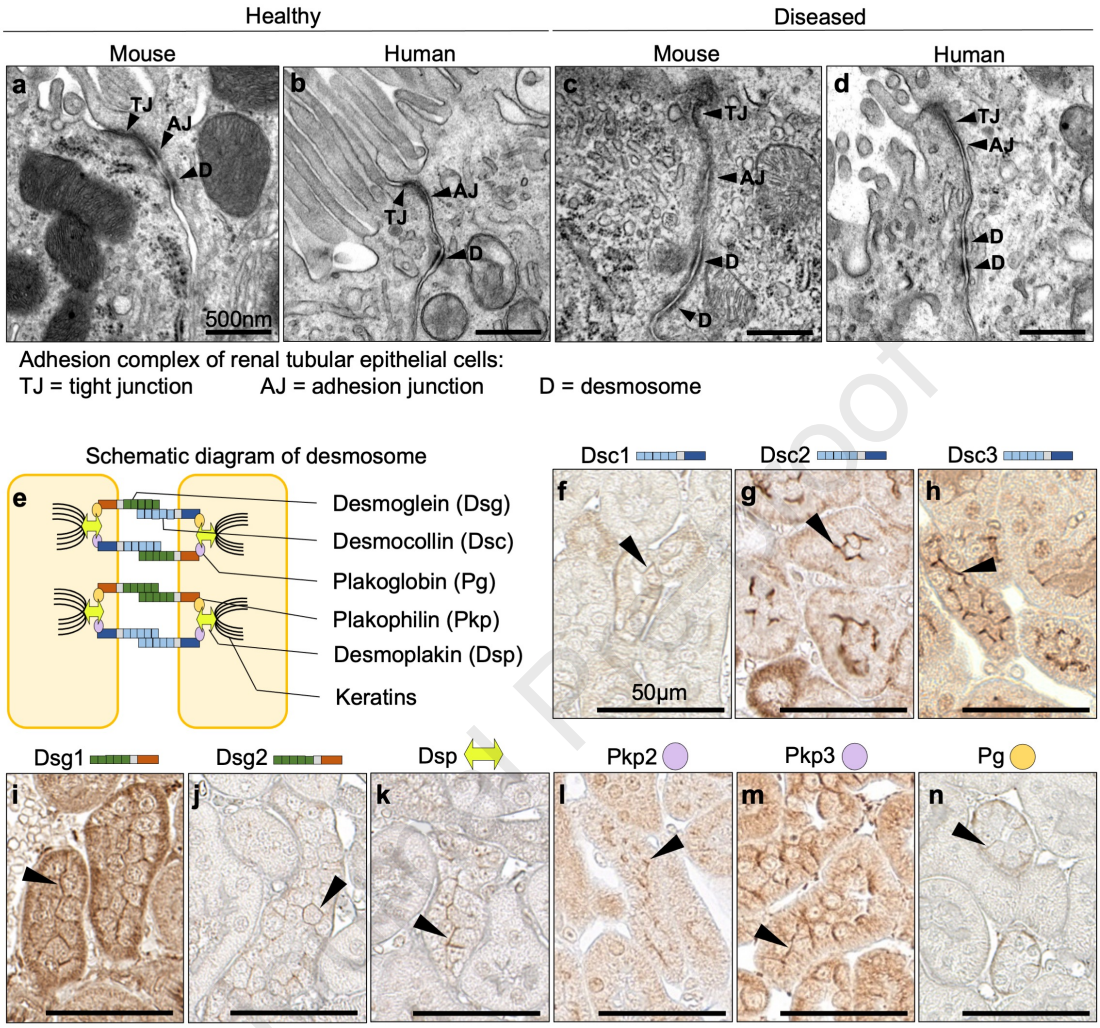
Healthy
Diseased
Mouse
Human
Mouse
Human
a
TJ
AJ
D
500nm
b
AJ
TJ
D
c
TJ
AJ
D
D
d
TJ
AJ
D
D
Adhesion complex of renal tubular epithelial cells:
TJ = tight junction
AJ = adhesion junction
D = desmosome
Schematic diagram of desmosome
e
Desmoglein (Dsg)
Desmocollin (Dsc)
Plakoglobin (Pg)
Plakophilin (Pkp)
Desmoplakin (Dsp)
Keratins
Dsc1
Dsc2
Dsc3
f
g
h
50μm
Dsg1
Dsg2
Dsp
Pkp2
Pkp3
Pg
i
j
k
l
m
n

Figure 2

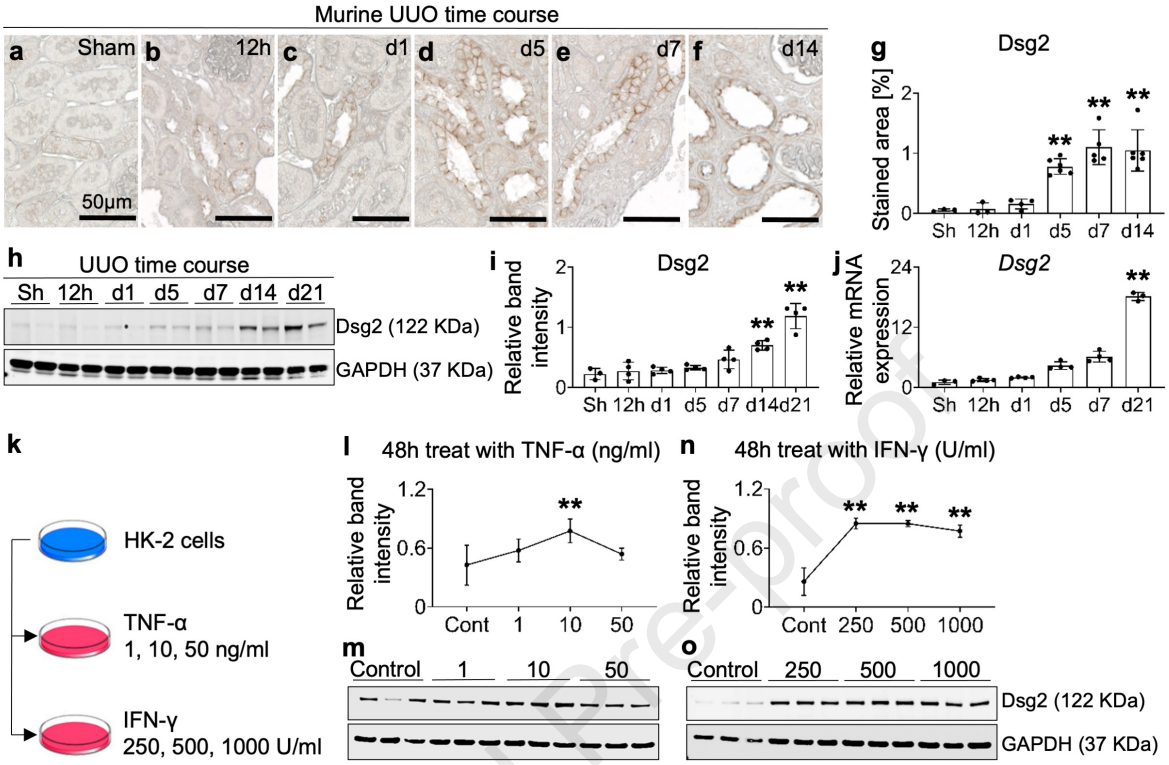

Figure 3

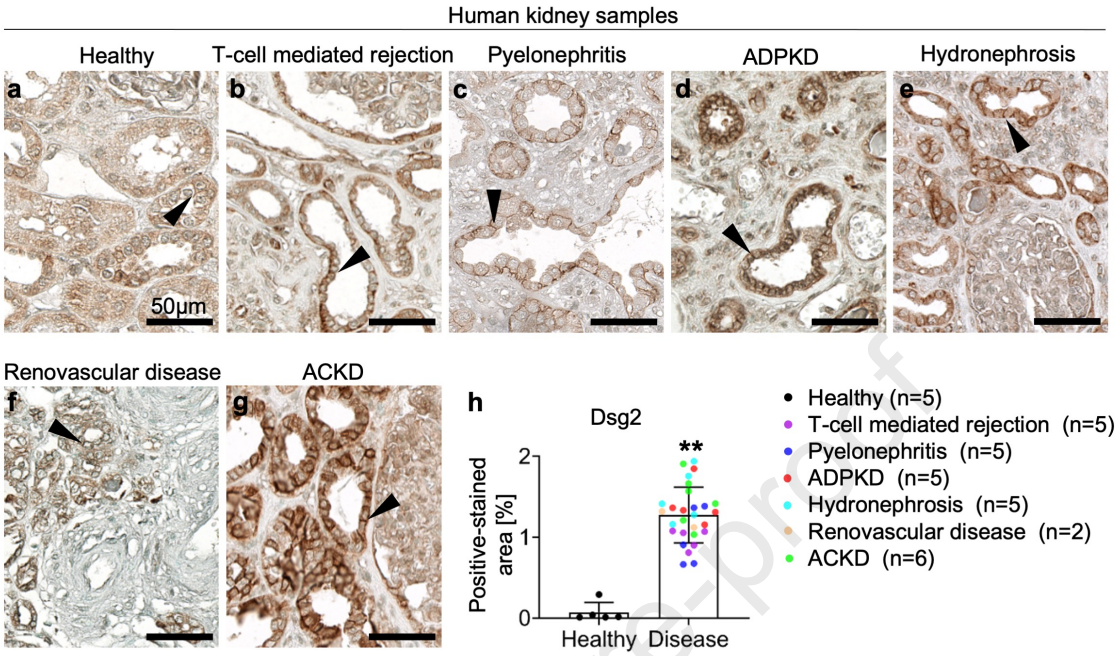

Figure 4

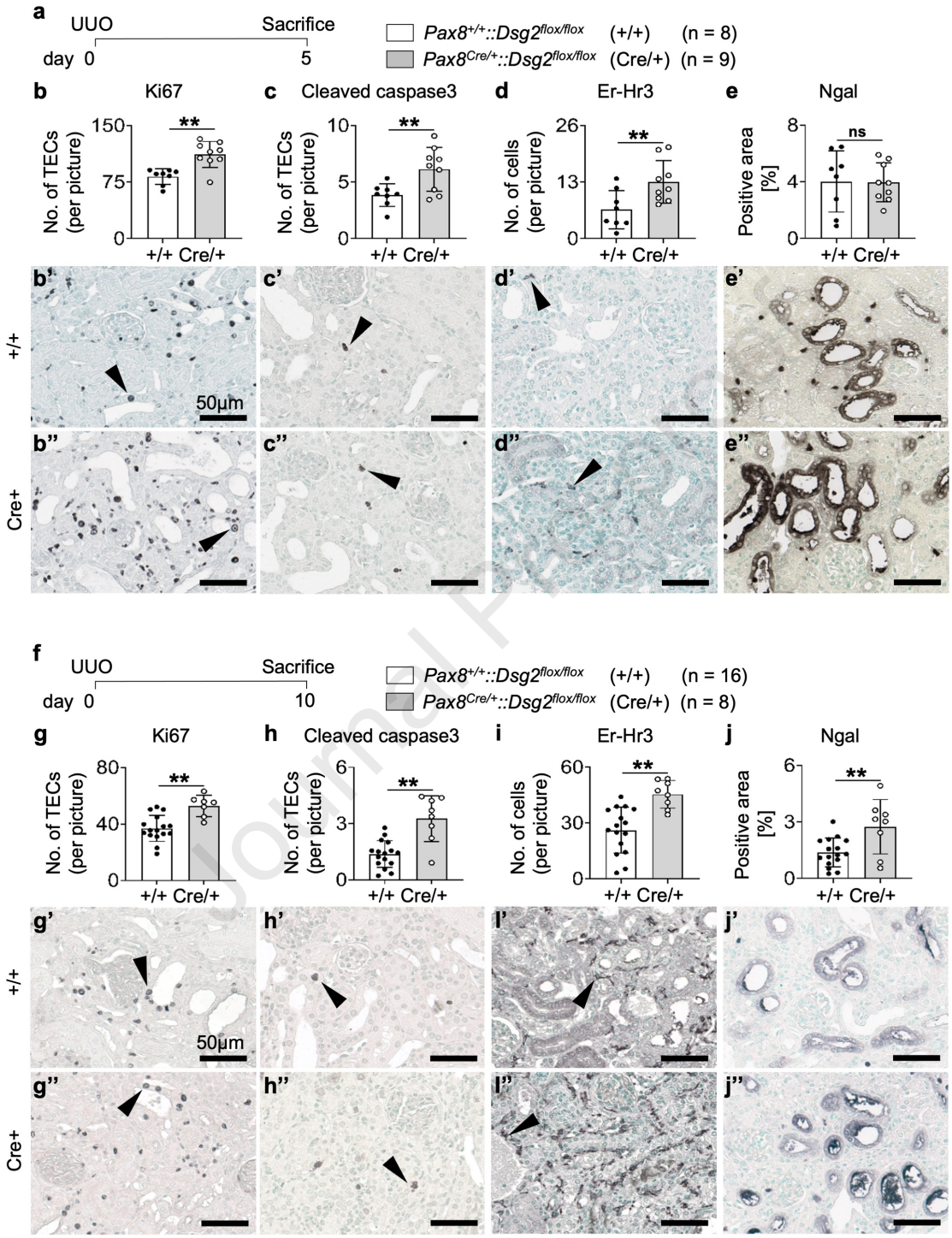
a
UUO
Sacrifice
day 0
5
Pax8+/+::Dsg2flox/flox (+/+) (n = 8)
Pax8Cre/+::Dsg2flox/flox (Cre/+) (n = 9)
b Ki67
c Cleaved caspase3
d Er-Hr3
e Ngal
No. of TECs (per picture)
No. of cells (per picture)
Positive area [%]
**
ns
+/+ Cre/+
b' c' d' e'
b'' c'' d'' e''
+/+
Cre+
50µm
f
UUO
Sacrifice
day 0
10
Pax8+/+::Dsg2flox/flox (+/+) (n = 16)
Pax8Cre/+::Dsg2flox/flox (Cre/+) (n = 8)
g Ki67
h Cleaved caspase3
i Er-Hr3
j Ngal
g' h' i' j'
g'' h'' i'' j''

Figure 5

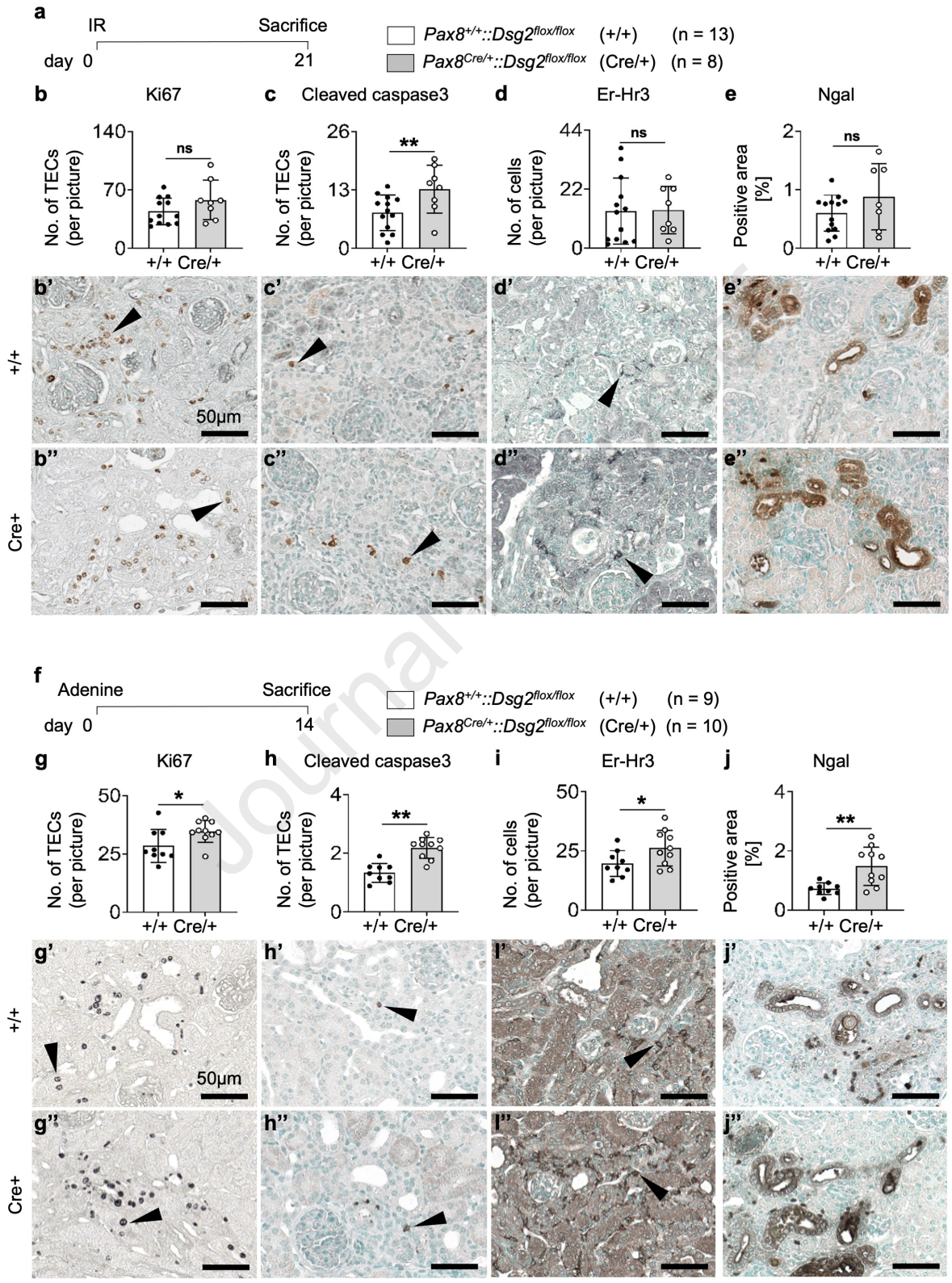
a
IR
Sacrifice
day 0
21
Pax8+/+::Dsg2flox/flox (+/+) (n = 13)
Pax8Cre/+::Dsg2flox/flox (Cre/+) (n = 8)
b Ki67
c Cleaved caspase3
d Er-Hr3
e Ngal
No. of TECs (per picture)
No. of cells (per picture)
Positive area [%]
ns
**
+/+ Cre/+
b' c' d' e'
b'' c'' d'' e''
+/+
Cre+
50µm
f
Adenine
Sacrifice
day 0
14
Pax8+/+::Dsg2flox/flox (+/+) (n = 9)
Pax8Cre/+::Dsg2flox/flox (Cre/+) (n = 10)
g Ki67
h Cleaved caspase3
i Er-Hr3
j Ngal
*
**
g' h' i' j'
g'' h'' i'' j''

Figure 6

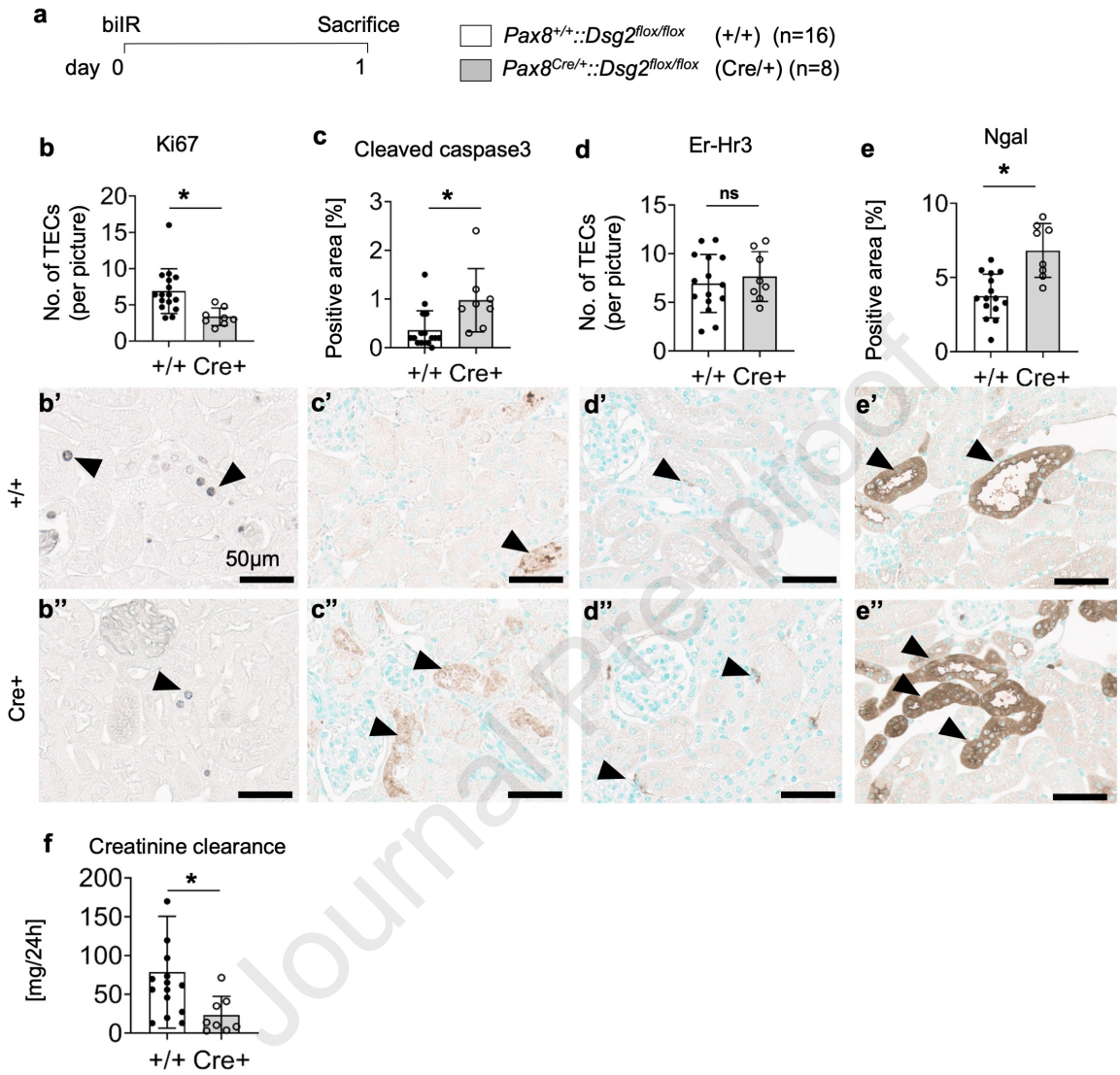

Figure 7

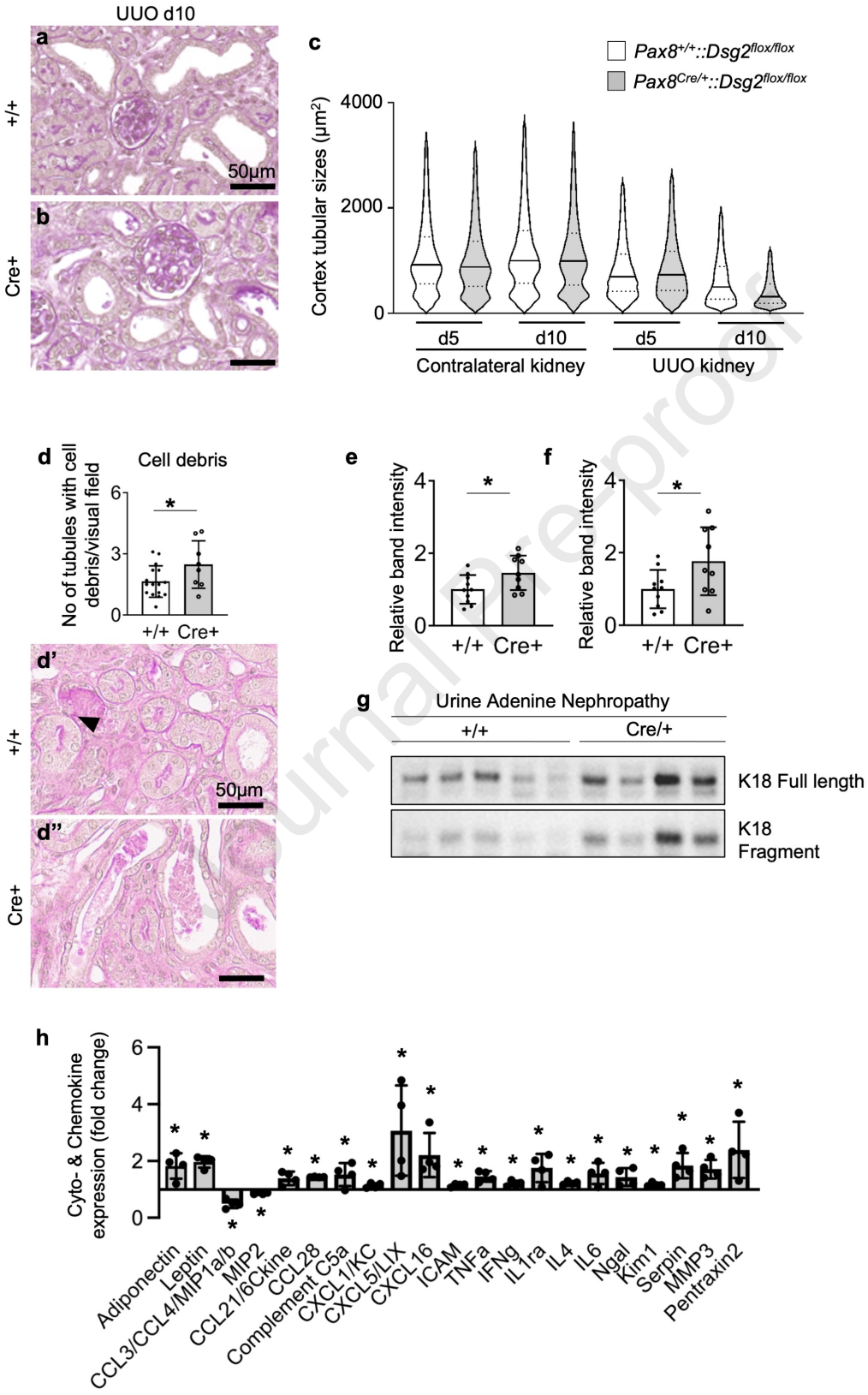
UUO d10
a
+/+
50μm
b
Cre+
c
Pax8+/+::Dsg2flox/flox
Pax8Cre/+::Dsg2flox/flox
Cortex tubular sizes (μm2)
4000
2000
0
d5
d10
d5
d10
Contralateral kidney
UUO kidney
d
Cell debris
No of tubules with cell debris/visual field
6
3
0
*
+/+ Cre+
d'
+/+
50μm
d''
Cre+
e
Relative band intensity
4
2
0
*
+/+ Cre+
f
Relative band intensity
4
2
0
*
+/+ Cre+
g
Urine Adenine Nephropathy
+/+
Cre/+
K18 Full length
K18 Fragment
h
Cyto- & Chemokine expression (fold change)
6
4
2
0
Adiponectin
Leptin
CCL3/CCL4/MIP1a/b
MIP2
CCL21/6Ckine
CCL28
Complement C5a
CXCL1/KC
CXCL5/LIX
CXCL16
ICAM
TNFa
IFNg
IL1ra
IL4
IL6
Ngal
Kim1
Serpin
MMP3
Pentraxin2

Figure 8